한국압력기기공학회 논문집
제15권 제1호 2019년 6월 pp. 18-27

ISSN 1738-8333
http://dx.doi.org/10.20466/KPVP.2019.15.1.018

<연구논문>

Evaluation of APR1400 Steam Generator Tube-to-Tubesheet Contact Area Residual Stresses

Wycliffe Kiprotich KIPTISIA† and Ihn NAMGUNG*

(Received 26 November 2018, Revised 11 June 2019, Accepted 17 June 2019)

ABSTRACT

The Advanced Power Reactor 1400 (APR1400) Steam Generator (SG) uses alloy 690 as a tube material and SA-508 Grade 3 Class 1 as a tubesheet material to form tube-to-tubesheet joint through hydraulic expansion process. In this paper, the residual stresses in the SG tube-to-tubesheet contact area was investigated by applying Model-Based System Engineering (MBSE) methodology and the V-model. The use of MBSE transform system description into diagrams which clearly describe the logical interaction between functions hence minimizes the risk of ambiguity. A theoretical and Finite Element Methodology (FEM) was used to assess and compare the residual stresses in the tube-to-tubesheet contact area. Additionally, the axial strength of the tube to tubesheet joint based on the pull-out force against the contact joint force was evaluated and recommended optimum autofrettage pressure to minimize residual stresses in the transition zone given. A single U-tube hole and tubesheet with ligament thickness was taken as a single cylinder and plane strain condition was assumed. An iterative method was used in FEM simulation to find the limit autofrettage pressure at which pull-out force and contact force are of the same magnitude. The joint contact force was estimated to be 20 times more than the pull-out force and the limit autofrettage pressure was estimated to be 141.85MPa.

Key Words : APR1400 SG, SG tube-to-tubesheet expansion joint, SG tube-to-tubesheet contact pressure, SG joint axial strength, Pull-out force, Limit autofrettage pressure, MBSE.

Nomenclature

APR: Advanced Power Reactor
c: Tube-tubesheet clearance
D: Constant of integration
D_s: Equivalent sleeve diameter
E: Elastic modulus
F_c: Joint contact force
F_p: Pull-out force
K_s: Tubesheet outer to inner radius ratio
K_t: Tube outer to inner radius ratio
L: Tubesheet length
l_e: Tube expanded length
P: Pitch
P_c: Contact pressure
P_c^*: Residual contact pressure
P_{cm}: Maximum contact pressure
P_e: Expansion pressure
P_{emax}: Maximum expansion pressure
P_{eyc}: Tubesheet complete yield pressure
P_{eyf}: Tube total yield pressure
P_{eys}: Tubesheet initial yield pressure
P_{eyt}: Tube initial yield pressure
P_o: Outside pressure
r_a, r_b, r_c: Tube inner, interface, and outer radius respectively
R_a, R_b, R_c: Tubesheet equivalent sleeve inner, interface and outer radius

† KEPCO International Nuclear Graduate School
E-mail : inamgung@kings.ac.kr
Tel: (052) 712-7314
* Corresponding Author, KEPCO International Nuclear Graduate School

SCC: Stress Corrosion Cracking
SG: Steam Generator
SSAR: Standard Safety Analysis Report
U_{rs}: Tubesheet radial displacement
U_{rt}: Tube radial displacement
η: Ligament efficiency
ρ: Density
σ_r: Radial stress
σ_u: Ultimate strength
σ_y: Yield stress
σ_z: Axial stress
σ_θ: Hoop stress
υ: Poisson ratio
ε_r: Radial strain
ε_θ: Hoop strain
IDEF0: Integration Definition for Functional Modeling Zero
Inconel 690TT: Inconel 690 Thermally Treated

1. Introduction

Steam generators (SGs) are an integral part of nuclear plants and are used to transfer heat from the reactor coolant system to the secondary coolant system. In APR1400, the tubes are attached to the tubesheet by hydraulic expansion creating residual contact pressure between the tube and tubesheet hole. The functional requirement placed on the SG tube-tubesheet joint is to provide a barrier between the reactor coolant, which may be contaminated with radioactive fission products, and the environment. [1] The design of SGs is a complex system and system engineering is applied throughout the SG life cycle as it encompasses a holistic view of the design and analysis. Model-Based System Engineering (MBSE) is a coherent and comprehensive means of consistently arriving at a realizable system effectively and efficiently. The system analysis phase provides a rigorous basis of data and information for technical understanding to aid decision making across the entire SG life cycle. The process performs quantitative assessments and estimations, and results obtained serve as input into various technical decisions, providing confidence in the adequacy and integrity of the system of the system definition towards achieving the appropriate system balance. [2] This paper focuses on system analysis phase of the SG life cycle to estimate the contact pressure, evaluate joint axial strength and find the limit autofrettage pressure at which pull-out force and joint contact force are of the same magnitude. The system analysis phase cycle is illustrated in Fig. 1. The present paper highlights the system engineering processes used to analyze residual stresses in the tube-tubesheet joint.

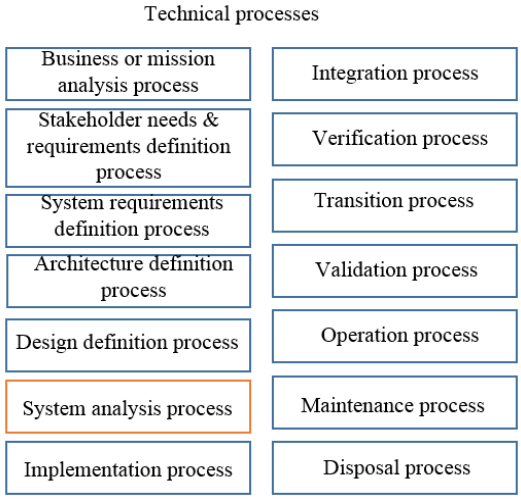

Fig. 1 System analysis phase in the system life cycle

2. Methodology

The V-model is used in the entire SG project execution as it ensures maximum transparency for all project participants. It is a systematic approach used to map requirements to process definitions. The V-model also performs reviews on multiple levels by tracing all

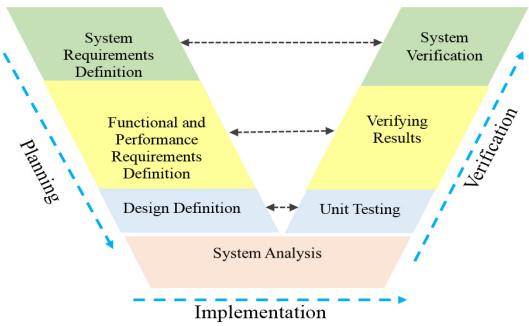

Fig. 2 V-model for SG life cycle

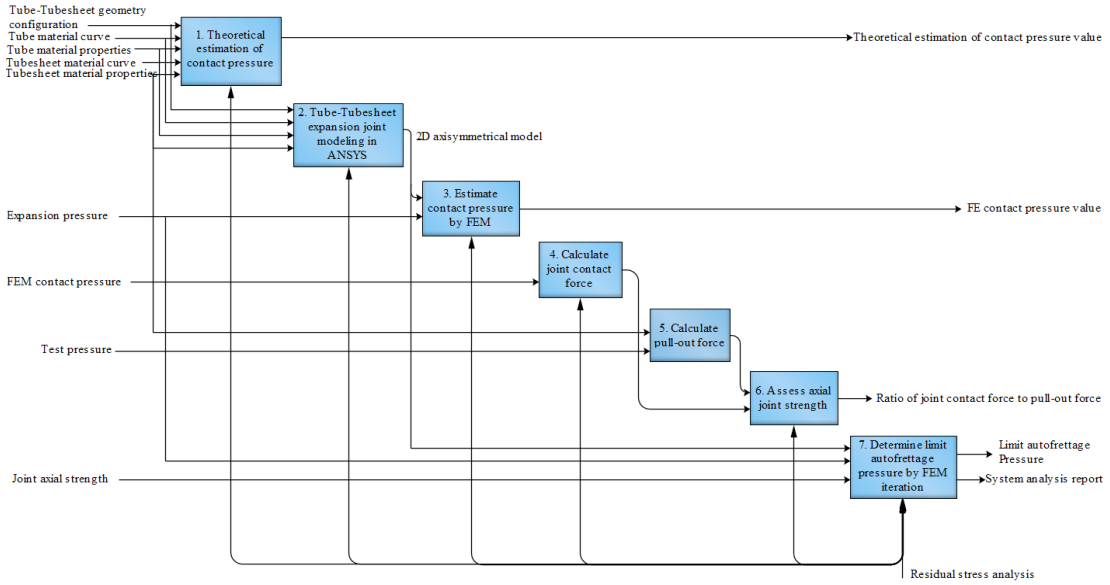

Fig. 3 IDEF0 diagram

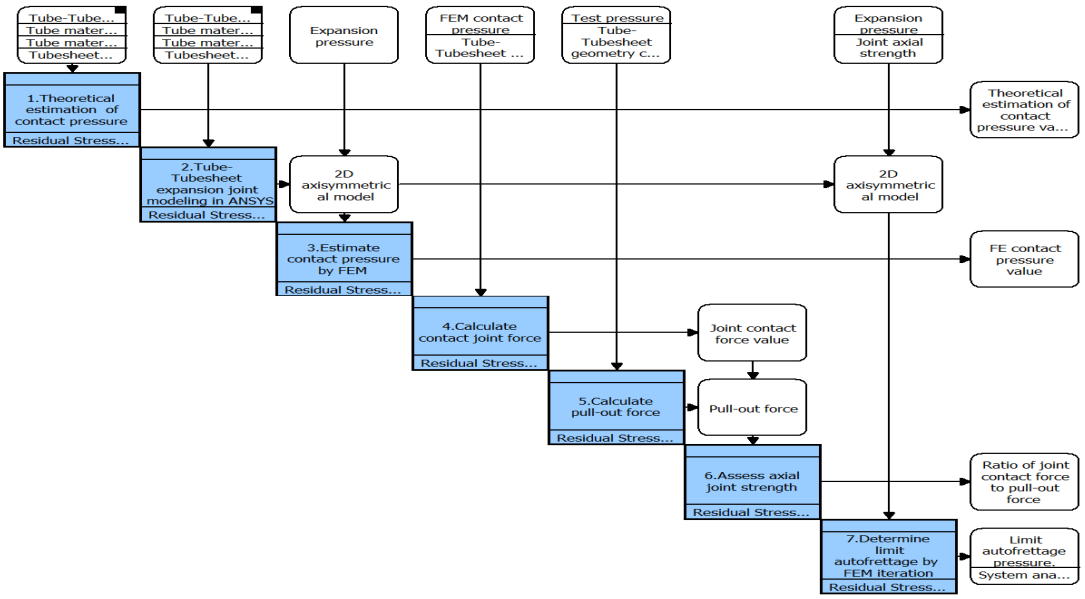

Fig. 4 N^2 diagram

requirements throughout the entire life cycle so as to ensure clear and unambiguous implementation of requirements.[3] Fig. 2 illustrates the V-model for SG life cycle. Integration Definition for Functional Modeling Zero (IDEF0) diagram and N Square Diagram (N^2) are used in this study to track the interdependencies of the various functions, inputs, and outputs as illustrated in Fig. 3 and Fig. 4. Enhanced Functional Flow Block Diagram (EFFBD) was then developed to relate the inputs and outputs through functional decomposition and provide a logical flow between the system functions as demonstrated in Fig. 5. It characterizes the flow of information among functions.

Table 1 Tube and tubesheet geometry specifications (1)

r_a(mm)	r_c(mm)	R_a(mm)	R_c(mm)	c (mm)	P(mm)	L (mm)
8.455	9.525	9.626	18.21	0.1016	25.4	647.7

Table 2 Material properties of Inconel 690TT and SA-508 Grade 3 Class 1 (5) (6)

Tube material	σ_y(MPa)	σ_u(MPa)	E(MPa)	υ	ρ(kgm^{-3})	Temperature
Alloy 690TT	275	686	207000	0.31	8110	25°C
Tubesheet material	σ_y(MPa)	σ_u(MPa)	E(MPa)	υ	ρ(kgm^{-3})	Temperature
SA-508 Gr.3 Cl. 1	501.34	1187	191000	0.3	7833.4	25°C

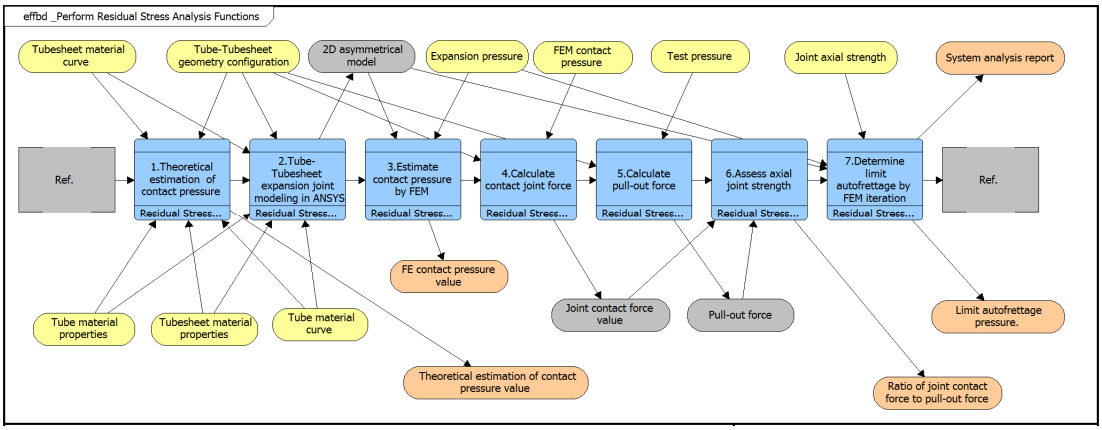

Fig. 5 EFFBD diagram

2.1 Theoretical development of contact pressure

The theoretical development of contact pressure is based on Elastic Perfectly Plastic (EPP) material behavior of both tube and tubesheet. Tube and tubesheet geometry specifications and material properties are given in Table 1 and Table 2 respectively. The method of calculating the residual contact stress is based on equilibrium and compatibility equations of thick-walled cylinder for the case of plane strain using von Mises yield criterion. [4] The elastic-plastic analysis of the large-strain cylinder can be analyzed by dividing the cylinder into plastic region ($r_a \le r \le r_b$) and elastic region ($r_b \le r \le r_c$) as shown in Fig. 6.

In the theoretical development of residual contact pressure, the following boundary conditions hold;

$$\sigma_r|_{r=r_a} = -P_e$$
$$\sigma_r|_{r=r_b} = -P_c$$
$$\sigma_r|_{r=r_c} = -P_o = 0$$

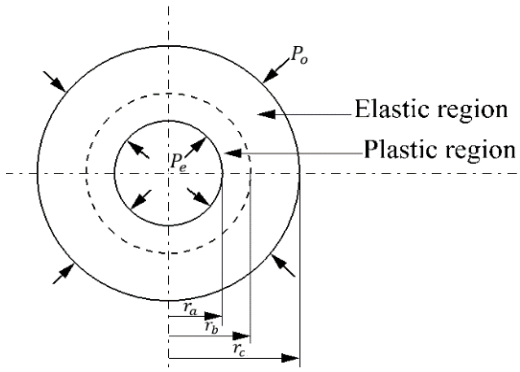

Fig. 6 Elastic and plastic regions in thick-walled cylinder

Equation (1) and (2) below give the radial force equilibrium and compatibility equations of thick-walled cylinders.

$$\frac{d\sigma_r}{d_r} + \frac{\sigma_r - \sigma_\theta}{r} = 0 \quad (1)$$

$$r\frac{d\varepsilon_\theta}{d_r} = \varepsilon_r - \varepsilon_\theta \quad (2)$$

The stresses in the elastic region are given by Lame' equations[4],

$$\sigma_r = \frac{r_b^2 P_c - r_c^2 P_o}{r_c^2 - r_b^2} - \frac{(P_c - P_c) r_b^2 r_c^2}{r^2 (r_c^2 - r_b^2)} \quad (3)$$

$$\sigma_\theta = \frac{r_b^2 P_c - r_c^2 P_o}{r_c^2 - r_b^2} + \frac{(P_c - P_c) r_b^2 r_c^2}{r^2 (r_c^2 - r_b^2)} \quad (4)$$

Stresses in the plastic region ($r_a \leq r \leq r_b$) can be derived as illustrated below;

From von Mises yield criterion, yielding of the inner surface due to expansion pressure, P_e occurs when,

$$\sigma_y = \sqrt{\frac{1}{2}[(\sigma_\theta - \sigma_r)^2 + (\sigma_r - \sigma_z)^2 + (\sigma_z - \sigma_\theta)^2} \quad (5)$$

For plain strain condition,

$$\sigma_z = \frac{1}{2}(\sigma_\theta + \sigma_r) \quad (6)$$

Substituting equation (6) into (5) gives von Mises equivalent stress,

$$\sigma_y = \frac{\sqrt{3}}{2}(\sigma_\theta - \sigma_r) \quad (7)$$

Substituting equation (8) above into the equilibrium equation (1) gives:

$$\frac{d\sigma_r}{d_r} = \frac{2}{\sqrt{3}} \frac{\sigma_y}{r} \quad (8)$$

Integrating both sides of the equation gives:

$$\sigma_r = \frac{2\sigma_r}{\sqrt{3}} lnr + D$$

The constant D can be obtained from the interface boundary conditions; at $r = r_b,\ \sigma_r = -P_c$

$$D = -P_c - \frac{2\sigma_y}{\sqrt{3}} lnr_b$$

Therefore,

$$\sigma_r = -P_c + \frac{2\sigma_y}{\sqrt{3}} ln \frac{r}{r_b} \quad (9)$$

Contact pressure, P_c can be determined from the following boundary conditions,

At $r = r_b,\ \sigma_r = -P_c$ and at $r = r_c,\ \sigma_r = -P_o$

At the elastic plastic interface, $r = r_b$, the Lame' solution and the yielding prevail simultaneously. Therefore, the contact pressure at which plastic deformation occurs at the interface is given by equation (7) above.

Substituting σ_r and σ_θ from equation (3) and (4) respectively into equation (7) and solving gives;

$$\frac{\sigma_y}{\sqrt{3}} = \frac{r_b^2 / r^2 (P_c)}{(r_c^2 - r_b^2)/r_c^2}$$

$$P_c = \frac{\sigma_y}{\sqrt{3}} \left[1 - \frac{r_b^2}{r_c^2}\right] \quad (10)$$

Substituting P_c into equation (9) and noting that at, $r = r_b,\ \sigma_r = -P_c$ gives,

$$\sigma_r = \frac{\sigma_y}{\sqrt{3}} \left(-1 + \frac{r_b^2}{r_c^2} + 2ln \frac{r}{r_b}\right) \quad (11)$$

The above equation is for determining radial stress at any radius r in the plastic region.

To find the relationship between P_e and elastic-plastic interface radius r_b, recall that at $r = r_a,\ \sigma_r = -P_e$

$$P_e = \frac{\sigma_y}{\sqrt{3}} \left(\frac{1 - r_b^2}{r_c^2} - 2ln \frac{r_a}{r_b}\right) \quad (12)$$

2.1.1 Tube-tubesheet configuration

Using the theoretical derivations above and applying to an actual tube-tubesheet configuration with clearance as shown in Fig. 7, the residual contact pressure can hence be determined. The behavior of the tube and tubesheet under hydraulic expansion is presented as follows;

2.1.2 Tube elastic-plastic deformation

Under the effect of the expansion pressure P_e, the pressure that causes a plastic zone of radius r_b in the tube is expressed by equation (12) above. The tube deforms elastically until the expansion pressure P_e reaches the value of P_{evt}, the pressure at which yielding of the tube starts. Initial yielding is calculated from equation (12) by letting $r_b = r_a$

$$P_{eyt} = \frac{\sigma_y}{\sqrt{3}}\left(1 - \frac{r_a^2}{r_c^2}\right) \tag{13}$$

Total yield occurs when $r_b = r_c$

$$P_{eyf} = \frac{2\sigma_y}{\sqrt{3}} ln \frac{r_a}{r_c} \tag{14}$$

For EPP materials, no increase in the expansion pressure beyond P_{evf} is necessary to close the gap and the displacement evolves independently until contact with tubesheet.

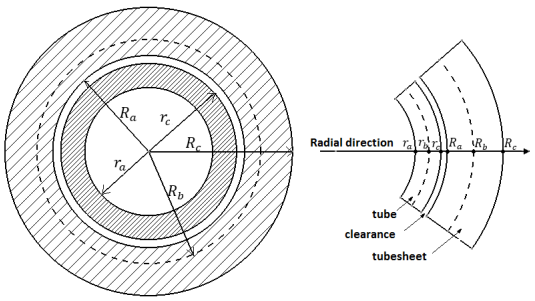

Fig. 7 Tube-tubesheet geometry configuration

2.1.3 Elastic deformation of tubesheet

After the contact has been made, the tubesheet will deform elastically by undergoing the same displacement at its inner radius as the tube outside radius minus the clearance. A contact pressure P_c build up at the interface. From geometrical compatibility equation,

$$u_r^t(r_c) = c + u_r^s(R_a) \tag{15}$$

Further increase in pressure, continues to deform the tube plastically while at the same time the tubesheet deforms elastically. A contact pressure P_c is created at the interface with a maximum value of P_{cm} at the maximum expansion,. P_{emax}, The expansion pressure P_{emax} is increased just up to start of tubesheet yield which is given by equation (13) by replacing r_a with R_a and r_c with R_c

$$P_c = \frac{\sigma_y}{\sqrt{3}}\left(1 - \frac{R_a^2}{R_c^2}\right) \tag{16}$$

The pressure required to cause the start of yield in tubesheet P_{evs} is given by equation (17) below,

$$P_{eys} = P_{eyf} + P_c \tag{17}$$

The expansion pressure required to cause complete plastic deformation of the tubesheet is given by equation (14) by replacing r_a with R_a and r_c with R_c

$$P_{eyc} = \frac{2\sigma_y}{\sqrt{3}} ln \frac{R_a}{R_c} \tag{18}$$

$$P_{esc} = P_{eyc} + P_{eyf} \tag{19}$$

However, increasing the expansion pressure beyond the elastic limit of the tubesheet will affect its structural integrity and also permanently enlarged holes could make retubing difficult.

2.1.4 Unloading Process

After reaching the maximum value P_{emax}, the release of pressure results in simultaneous elastic recovery of the tube and the tubesheet. Therefore, the contact pressure is determined by evaluating the change in radial displacement of both the tube and tubesheet at their interface. [7] From geometrical compatibility equation,

$$\triangle u_r^t(r_c) = \triangle u_r^2(R_a) \tag{20}$$

During unloading, the tube relative displacement is given by the elastic recovery from where it is subjected to the maximum internal pressures P_{emas} and P_{cmax}

and a lower state level where it is subjected to the internal and external pressures P_e and P_c.

$$\triangle u_r^t(r) = \frac{3rP_e}{2E_t(K_t^2-1)} \tag{21}$$

$$\triangle u_r^t(r) = \frac{3r}{2E_t(K_t^2-1)}[(P_e - P_{emax}) - (P_c - P_{cmax})]$$

The tubesheet relative displacement is given by the elastic recovery from where it is subjected to the maximum pressure P_{cmax} to the lower value P_c.

$$\triangle u_r^s(r) = \frac{3rK_s^2P_e}{2E_s(K_s^2-1)}$$

$$\triangle u_r^s(r) = \frac{3K_s^2r}{2E_s(K_s^2-1)}(P_c - P_{cmas}) \tag{22}$$

Substitute equation (21) and (22) into equation (20) and evaluate at $r_c$and r_a respectively,

$$\frac{er_c}{2E_t(K_t^2-1)}[(P_e - P_{emax}) - (P_c - P_{cmax})]$$
$$= \frac{3K_s^2R_a}{2E_s(K_s^2-1}(P_c - P_{cmas})$$

$$\frac{r_c}{E_t(K_t^2-1)}[(P_e - P_{emax}) - (P_c - P_{cmax})]$$
$$= \frac{K_s^2R_a}{E_s(K_s^2-1)}(P_c - P_{cmas})$$

Let $E_s(K_s^2-1)$ be X

Let $E_t(K_t^2-1)$ be Y

$$Xr_c[(P_e - P_{emax}) - (P_c - P_{cmax})]$$
$$= YK_x^2R_a(P_c - P_{cmax})$$

$$P_c = P_{cmax} + \frac{Xr_o(-P_{emax})}{(YK_s^2R_a + Xr_c)} \tag{23}$$

Residual contact pressure P_c^* is given by putting P_e in equation (24) equal to zero.

$$P_c = P_{cmax} + \frac{Xr_o(P_e - P_{emax})}{(YK_s^2R_a + Xr_c)} \tag{24}$$

2.2 Theoretical assessment of joint axial strength

Joint axial strength is the axial force required to break the bond between tube and tubesheet. The joint contact force is due to a shearing force acting between the tube and tubesheet and exists as a result of the residual contact pressure. In this study, the pull-out force due to internal test pressure 21.417MPa is calculated and measured against the joint contact force. The joint contact force is proportional to the expanded area of the tube and the residual contact pressure. The joint contact force is given by the formula below, [8]

$$F_c = 2\pi r_c l_e f P_c^* \tag{25}$$

Where,

f is a frictional interaction between SA-508 and alloy 690TT material and was determined experimentally by Allam and Bazergui as 0.1375. [8] It is an essential input data in FEM analysis as it affects the reliability of the results.

l_e is expanded length of the tube within the tubesheet.

The pull-out force due to internal test pressure is calculated from equation (26) below,

$$F_p = \pi r_c^2 P_t \tag{26}$$

An iterative method in FEM simulation was then used to find the optimum autofrettage pressure at which pull-out force and contact joint force are of the same magnitude. A 10% conservatism was factored in the analysis due to uncertainties during the expansion process as illustrated in equation (27) below. Seal welding of the tubes on the cladding that also contributes to the strength of the joint was not considered in the present study.

$$\delta = F_c - 1.1F_p \tag{27}$$

The test pressure was chosen in this study because it is the highest pressure the SG is tested (cold hydro test). During operation of the steam generator, the test pressure value cannot be reached as the pressurizer safety valve operates at 17.099MPa hence optimizing the expansion pressure at test pressure value will result in a strong and safe joint.

3. Finite Element Analysis

The Finite Element Method (FEM) is used to estimate the residual contact pressure resulting from hydraulic expansion process and determine limit autofrettage pressure.

3.1 Geometry of the model

In this analysis, the tubesheet is modeled by an equivalent sleeve diameter that produces the same results as on actual tubesheet configuration. [9] Fig. 7 shows the tube and tubesheet geometry configuration. Tubesheet equivalent sleeve diameter is calculated as shown below,

$$\frac{D_s}{P_t} = 12.55\eta^5 - 16.2181\ \eta^4 + 10.88288\ \eta^{3-}$$
$$2.43388\ \eta^2 + 1.94683\ \eta + 0.98034 \qquad (28)$$

3.2 Material properties

The steam generator of APR1400 plants uses thermally treated alloy 690 as tube material and SA-508 Grade 3 Class 1 as tubesheet material. The material properties were obtained from ASME Code Section II [5] and APR1400 SSAR [1] and were appropriately defined in ANSYS for elastic-plastic analysis of tube and tubesheet. The material properties are as given in Table 2. The true stress-strain curves of the materials adopted in the present study are shown in Fig. 9 and Fig. 10.

3.3 Displacement boundary condition

In the 2D axisymmetric model, the front ends of the tube and tubesheet at the primary side through which uniform pressure is applied is constrained in the axial direction by applying frictionless support as shown in Fig. 8. Meshing was refined on the tube and contact area region where large deflections are expected to occur.

3.4 Loading condition

Specifying the proper loading conditions is key in non-linear FEM analysis. Non-linearities in this model arise due to contact non-linearity, material non-linearity, and geometry non-linearity. A uniform pressure of 250MPa was incrementally applied in multi-load steps because of large deformation involved especially when the tube plastic collapse is achieved. The pressure was then gradually released to zero thereby creating a residual contact pressure between tube and tubesheet. The pressure was applied 3mm below the tubesheet top surface to represent the space occupied by the hydraulic expander.

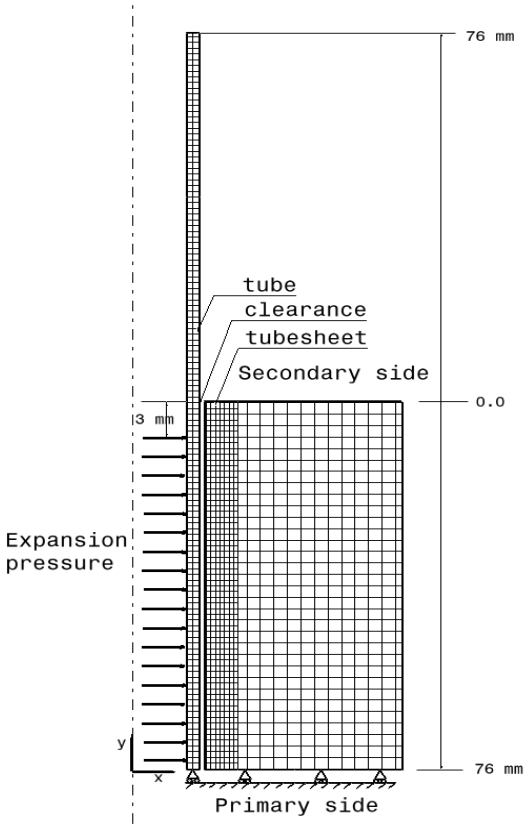

Fig. 8 2D axisymmetric model

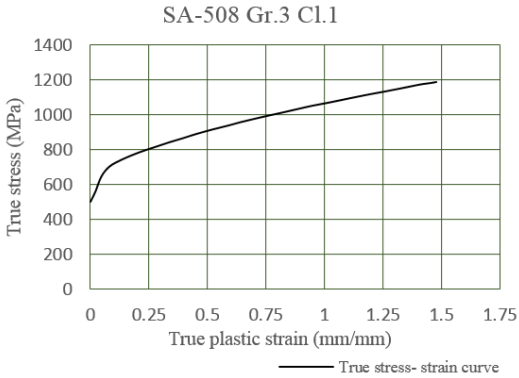

Fig. 9 SA-508 Gr.3 Cl.1 plastic stress-strain curve [6]

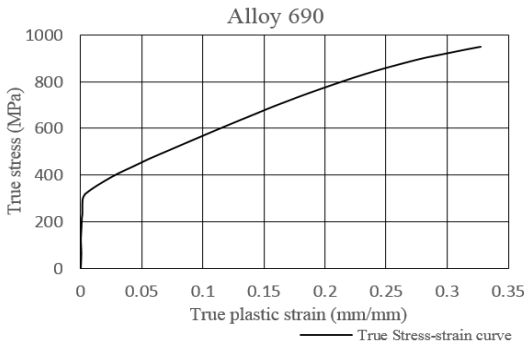

Fig. 10 Alloy 690 stress-strain curve [10]

4. Results and Analysis

In the FEM analysis, the contact pressure was determined at the end of the expansion process on the expanded zone where the value is constant, i.e. between -76mm and -40mm as shown in Fig. 11 below.

- From equations (1) to (24), the theoretical estimation of contact pressure was found to be 32.4MPa while the FEM estimates it to be 29.02MPa, the difference being 10%.
- From equations (25) and (26), the theoretical pull-out force was estimated to be 6,715kN while the contact force was estimated to be 138,98kN respectively. The contact force is 20 times higher than the pull-out force.
- The limit autofrettage pressure at which pull-out force and joint contact force are of the same magnitude was estimated to be 141.85MPa as illustrated in Fig. 12.

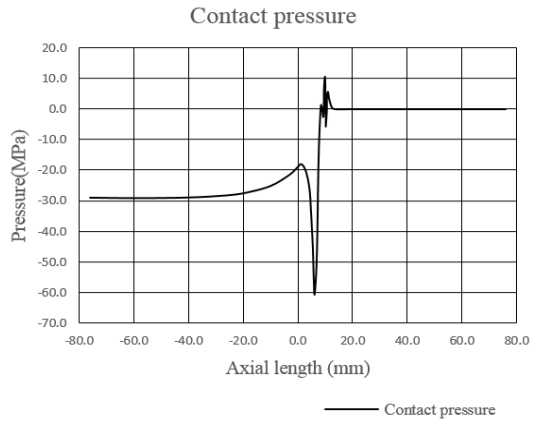

Fig. 11 Contact pressure distribution

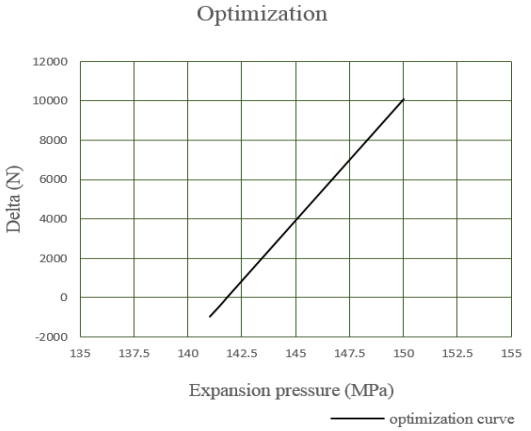

Fig. 12 Expansion pressure optimization

5. Discussion and Conclusion

This paper has demonstrated how system engineering processes were applied to analyze residual stresses in the tube-to-tubesheet contact area. V-model was applied to trace all requirements throughout the entire life cycle so as to ensure clear and unambiguous implementation of requirements. IDEF0 and N^2 diagrams were used to track the interdependencies of the various functions, inputs, and outputs in the study. EFFBD diagram was developed to define the functional decomposition and provide a logical flow of the various activities. In the study, theoretical analysis of the contact pressure was carried out and the results validated using FEM. FEM estimates contact pressure of 29.02MPa while theoretical estimation gives 32.4MPa. The joint contact force was estimated to be 20 times more than the pull-out force under test condition pressure of 21.417MPa. Iteration using FEM was carried out to find limit autofrettage pressure at which pull-out force and contact pressure are of the same magnitude. The limit pressure was estimated to be 141.85MPa. In this study Core 9 software was used as the system engineering tool.

Acknowledgment

Appreciation goes to Kepco International Graduate School (KINGS) for the support accorded in the completion of this project.

References

(1) Korea Electric Power Research Institute (KEPRI), 2014, *APR1400 SSAR - Chapter 5. Reactor coolant system and connected system*, Korea.

(2) INCOSE-TP-2003-002-04, 2015, *System Engineering Handbook, Guide for System Life Cycle Process and Activities,* 4th edition. John Wiley and Sons. Inc., Hoboken New Jersey, USA.

(3) Kossiakoff, A., Sweet, W. N., Seymour, S. J. and Biemer, S. M., 2003, *Systems Engineering Principles and Practice,* A John Wiley & Sons, Inc. Publication, New Jersey, USA.

(4) Harvey J. F., 1987, *Theory and design of pressure vessels,* Van Nostrand Reinhold Co., New York.

(5) ASME Boiler and Pressure Vessel Code, Sec. II, 2010, “Material Properties”, American Society of Mechanical Engineers, New York.

(6) Kweon H.D., Heo E.J., Lee H.D., and Kim J.W., 2018, "A methodology for determining the true stress-strain curve of SA-508 low alloy steel from a tensile test with fine element analysis," *Journal of Mechanical Science and Technology.,* Vol. 32, No. 7, pp. 3137-3143.

(7) Bouzid A. H., Mourad A. I. and Domiaty A. E., 2016, "Influence of Bauschinger effect on the residual contact pressure of hydraulically expanded tube-to-tubesheet joints," *International Journal of Pressure Vessel and Piping.,* Vol. 146, pp. 1-10.

(8) Allam M. and Bazergui A., 2002, "Axial Strength of Tube to Tubesheet Joints: Finite Element and Experimental Evaluations," *Journal of Pressure Vessel-Technology, ASME,* Vol. 124, No.1, pp.22-31.

(9) Kohlpaintner W. R., 1995, "Calculation of Hydraulically Expanded Tube-to-Tubesheet Joints," *Journal of Pressure Vessel-Technology, ASME,,* Vol. 117, No.1, pp. 24-30.

(10) Bergant, M., Yawny, A. and Perez-Ipina, J., 2017, "J-resistance curves for Inconel 690 and Incoloy 800 nuclear steam generators tubes at room temperature and at 300 °C," *Journal of Nuclear Materials,* Vol. 486, pp. 298-307.